Digital Design of Streamlined EMU Head Car and Its Smoothness Evaluation

Zhenfeng Wu, Zhoufeng Chen and Wangcai Ding

School of Mechanical ＆ Electrical Engineering，Lanzhou Jiaotong University，
Lanzhou，China
wzhf@mail.lzjtu.cn

Abstract

The outer shape of high-speed EMU（Electric Multiple Units）head car is formed by three-dimensional free surface. In view of the structural features of head, car，it can be divided into two parts, which are the driver cab and the compartment. This paper proposed a digital design method of EMU head car outer surface by adopting NURBS theory. We firstly created the main control lines by inputting control point coordinates and added the intermediate control lines to the main ones for the driver cab, meanwhile the control lines were optimized by adjusting the position of the control points. Finally，the reticular region, which formed by the main control lines and intermediate ones were padded. The outer shape of the compartment was stretched based on a two-dimensional sketch. The driver cab and the compartment were assembled in a virtual environment. The static evaluation of head car shows that the measured region has reached the surface smoothness requirements. The dynamic flow field analysis illustrates that the air trajectories which passing through the head car are smooth and natural, and be compared with a quasi-streamlined EMU，its total air resistance decreases significantly. This study will provide technical support for the subsequent process design and production control of high-speed EMU.

Keywords：NURBS；Streamlined EMU；Head car；Digital design；Smoothness evaluation；Aerodynamic analysis

1. Introduction

In recent years, with the constant construction and operation of intercity railways and passenger dedicated railways in China, they not only speed up traveling of people, make cities becoming closer, but also boost and balance the economic development of the areas which along the lines [1]. At present, the high-speed EMU (Electric Multiple Units) as the main type of vehicles has been widely used both in intercity railways and passenger dedicated railways. EMU is a kind of passenger train, which is composed of motor cars and trailer cars as a fixed marshalling. The broad application of high speed EMU indicates that China has entered the era of high-speed railway.

Some relevant researches indicated that air resistance in the proportion of the total resistance could reach more than 70% when EMU is running at the speed over 200km/h [2]. Based on this reason, the head car must adopt a streamlined outline in order to lower air resistance when EMU is running at high speeds. Besides, the EMU with a streamlined outline is also the embodiment of modernization and visualization of China's railway. Therefore, how to design the EMU head car with smooth surface and attractive appearance as well as meeting the aerodynamics requirements has become the focus of specialists in railway vehicle industry.

NURBS (Non-Uniform Rational B-Spline) is a widely popular method that can be used in free curve or surface modeling, and it introduces the concepts of weighted factor and

control point, which could provide some convenient factors for accurately completing complex surface products. Up to now, many efforts have been made towards developing NURBS method. Catmull and Clark [3] earlier proposed the conception of NURBS based on the B-Spline method. Pieg1 [4] introduced two methods to vary the shape of NURBS curve and surface: control point-based modification and weighted factor-based modification. Au and Yuen [5] proposed approaches that modify the shape of NURBS curve by altering the weighted factor and location of control points simultaneously. Zheng et al [6] presented a new approach that could directly manipulate the shape by modification in control points and knot refinement.Cherpea [7] and Ozbolat et al. [8] considered the common steps of NURBS curve and surface modeling. Huang [9] and Hu [10] discussed the application of NURBS method in the designing process of aircraft nose and V-shaped hull, respectively. Besides, NURBS method can also be applied in the field of CNC machining. Shen [11] proposed the least square approximation algorithm of NURBS curve with weighted factors，which could actualize the high-speed and smoothing milling of micro-segment.

At present, the NURBS method is mainly used in the field of automobile, airplane and home appliance, however, the studies about how to apply the NURBS method to complete the EMU head car are still rare. The objective of this paper is to present the design process of streamlined EMU head car by adopting NURBS method and carry out the static smoothness evaluation and dynamic aerodynamic analysis of the design results.

The paper is organized as follows: theoretical foundation of NURBS curve and surface is given in section 2. Section 3 presents the digital designing process of EMU head car. Multiple section curvature combs and reflection lines methods, which applied to evaluate the smoothness of head car are given in section 4. Section 5 presents the aerodynamic performance evaluation of the streamlined train and quasi-streamlined train in flow field. Conclusions of this paper are noted in Section 6.

2. Theoretical Foundation for NURBS Curve and Surface

The design process of industrial products surface often adopt the B spline method and Bezier method. Although the both methods may express parabolic curve and surface exactly, they can't express quadratic curve and surface exactly but approximately. The approximate expression will not only bring a lot of trouble for data processing, but also may arouse design errors that are inexistent [12].

The NURBS method is a perfect and all-purpose expression owing to it can exactly express the elementary curve (surface) and free curve (surface). Besides, the mathematical expressions of NURBS method include weighted factor and control point. It does not affect other parts when adjust local shape of the curve or surface by changing local control points and weighted factors, which could provide greater flexibility for complex surface products. In consideration of the advantages of the NUBRS method, the ISO (International Organization for Standardization) put it as the only mathematical method for defining industrial product geometry in STEP (Standard for the Exchange of Product model data) in 1991 [13].

2.1 Expression Method of NURBS Curve

A k order NUBRS curve can be defined as:

$$p(u) = \frac{\sum\limits_{i=0}^{n} w_i d_i N_{i,k}(u)}{\sum\limits_{i=0}^{n} w_i N_{i,k}(u)} \tag{1}$$

In formula (1), w_i ($i = 0,1,\cdots,n$) are called weighted factors, which are corresponding to the control points d_i ($i = 0,1,\cdots,n$). The weighted factors are equivalent to the "gravity" of the control points, the greater the value, the closer the curve to the control points [14]. Besides, in order to prevent the denominator equals zero in formula (1), it requires first weighted factor $w_0 > 0$ and last weighted factor $w_n > 0$, others $w_i \geq 0$. The influence of weighted factor on NURBS curve is shown in Figure 1.
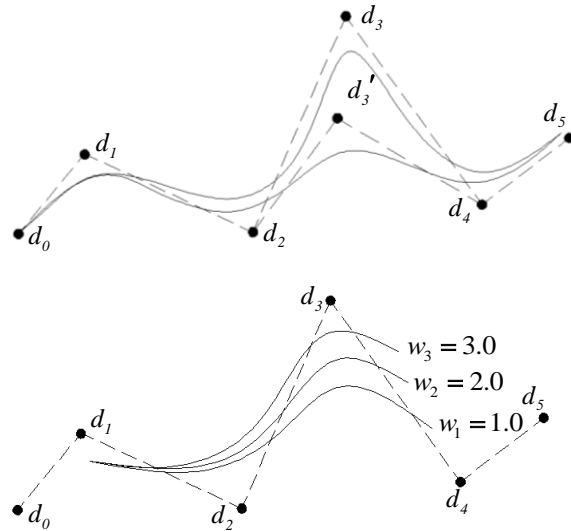

Figure 1. Influence of Weighted Factor on Curve

In formula (1), $d_i (i = 0,1,\cdots,n)$ are called control points which are usually not on the curve, but the shape of NURBS curve is determined by the control polygon formed by them. The shape of the NURBS curve can be changed by dragging the control point and the effect is shown in Figure 2.
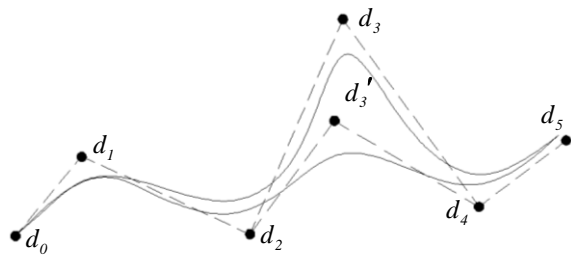

Figure 2. Influence of Control Point on Curve

In formula (1), $N_{i,k}(u)$ is described as the base function of B spline curve. It is defined as follows: taking $u_0,u_1,\cdots,u_{n+k+1}$ knots to form vector U, so $U = \{u_0,u_1,\cdots,u_{n+k+1}\}$, the base function can be written as formula (2) ~ (4).

$$N_{i,0}(u) = 1 , \quad u_i \leq u \leq u_{i+1} \tag{2}$$

$$N_{i,0}(u) = 0 , \quad u < u_i \text{ or } u > u_{i+1} \tag{3}$$

$$N_{i,k}(u) = \frac{u - u_i}{u_{i+k} - u_i} N_{i,k-1}(u) + \frac{u_{i+k+1} - u}{u_{i+k+1} - u_{i+1}} N_{i+1,k-1}(u) \tag{4}$$

In formula (4), k is the order of the B spline curve. To ensure the second derivative of B spline curve is continuous, it needs to take $k \geq 3$, u and i are the knot and the serial number of the B spline curve, respectively.

2.2 Expression Method of NURBS Surface

A $k \times l$ order NURBS surface can be expressed as:

$$P(u,v) = \frac{\sum_{i=0}^{m}\sum_{j=0}^{n} w_{i,j} d_{i,j} N_{i,k}(u) N_{j,l}(v)}{\sum_{i=0}^{m}\sum_{j=0}^{n} w_{i,j} N_{i,k}(u) N_{j,l}(v)} \qquad (5)$$

In formula (5), $w_{i,j}$ ($i = 0,1,\cdots,m$, $j = 0,1,\cdots,n$) are called the weighted factors, which are corresponding to the control points $d_{i,j}$. They have the effect of stretching and compressing to a control point on curved surface. $d_{i,j}$ ($i = 0,1,\cdots,m$, $j = 0,1,\cdots,n$) are the control points of space network. $N_{i,k}(u)$ ($i = 0,1,\cdots,m$) and $N_{j,l}(v)$ ($j = 0,1,\cdots,n$) are base functions of B spline surface，which are k order in u direction and l order in v direction, respectively. The define method of $N_{i,k}(u)$ is totally the same as formula (4). $N_{j,l}(v)$ is defined as formula (6).

$$N_{j,l}(v) = \frac{v - v_j}{v_{j+l} - v_j} N_{j,l-1}(v) + \frac{v_{j+l+1} - v}{v_{j+l+1} - v_{j+1}} N_{j+1,l-1}(v) \qquad (6)$$

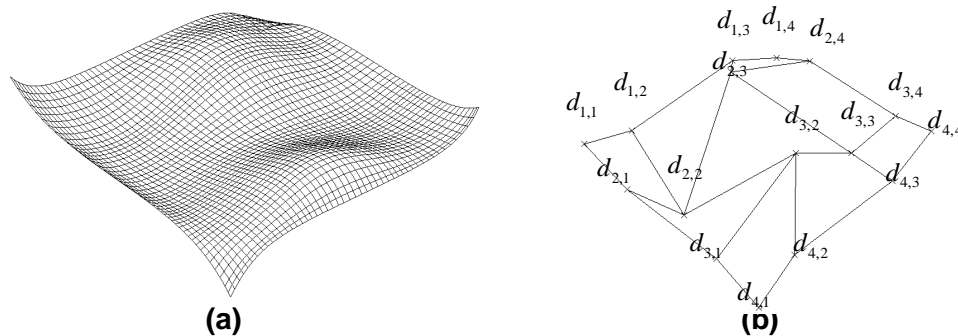Figure 3 is a free form NURBS surface and its grids which formed by the control points.

Figure 3. Free Form NURBS Surface: (A) Space Shape of the Surface (B) Control Points of the Surface

3. Surface Design of EMU Head Car

In order to effectively reduce the air resistance and the strength of pressure waves when train is running at high speed, the head car of high-speed EMU should be generally designed with a streamlined shape. Because the head car is longer and its outer shape is complex, we may design the driver cab and the compartment respectively, and assemble the two parts in a virtual environment.

CATIA is a kind of three-dimensional software developed by Dassault System Company of France, which includes the functions CAD, CAE and CAM [15]. It can

complete all the process of product design such as concept design, detailed design, engineering analysis and virtual manufacturing, etc. Because CATIA completely supports the method of NURBS curve and surface, the design process of EMU head car involved in this paper is finished by adopting it.

3.1 Coordinate System of the Model

A proper coordinate system must be set before the design process and its setting principle is as follows: the upper plane of railway track is xy plane，and the projection point of the nasal tip of head car, which is on the xy plane, is the coordinate origin and named O. The windward direction of EMU is the positive direction of the x-axis. The direction, which is vertical, upward and starting from point O, is the positive direction of the z-axis. The positive direction of the y-axis is decided by the right-hand rule. The coordinate system of head car model is shown in Figure 4.
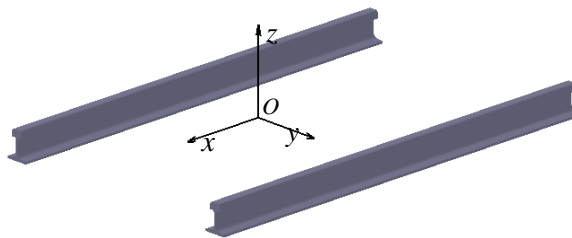
Figure 4. Coordinate System of the Model

3.2 Main Control Lines of Driver Cab

In this paper, the driver cab adopts a double arch surface, i.e. the region of head car nose is smooth and the remaining region of the surface have a smooth transition with no obvious protrusions. As the driver cab has a high degree of symmetry, it only needs to accomplish half model of the driver cab in longitudinal direction and complete the total model by symmetry operation.

To express the shape characteristics of the driver cab completely, firstly we need to input three-dimensional coordinates of control point's d_i ($i = 0,1,\cdots,n$)of the maximum longitudinal symmetry control line one by one in the "Generative Shape Design" workbench of CATIA software, and then generates NURBS curve with control points. Finally, the shape of maximum longitudinal symmetry control line is determined by adjusting the first and the end curve tangent vector V_1 and V_2, respectively. The finished maximum longitudinal symmetry control line is shown in Figure 5. The maximum overlooking control line, cross-sectional contour lines and adjustable lines are finished by repeating the steps mentioned above.
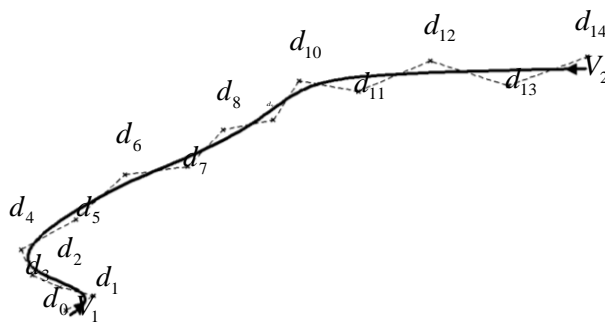
Figure 5. Maximum Longitudinal Symmetry Control Line

The half-digital model of the driver cab is formed by 17 control lines, totaling 206 control points. The rearmost cross section of the driver cab includes 15 control points, and their coordinates are listed in Table 1.

Table 1. Coordinates Of Control Points at the Rearmost Cross Section of Driver Cab (Unit: Mm)

Point number	X	Y	Z
1	-9500.0	0	3700.0
2	-9500.0	353.036	3692.207
3	-9500.0	706.921	3668.705
4	-9500.0	1076.429	3627.250
5	-9500.0	1354.052	3568.260
6	-9500.0	1562.466	3327.587
7	-9500.0	1614.329	2998.788
8	-9500.0	1640.829	2599.811
9	-9500.0	1668.942	2176.553
10	-9500.0	1683.503	1947.148
11	-9500.0	1686.265	1743.892
12	-9500.0	1677.667	1355.647
13	-9500.0	1677.612	971.226
14	-9500.0	1607.308	531.892
15	-9500.0	1399.992	200.000

Besides, all the main lines should be faired, and the maximum deviation value should be within 0.001mm. This step is the key to express the surface shape of the driver cab and the finished main control lines are shown in Figure 6.
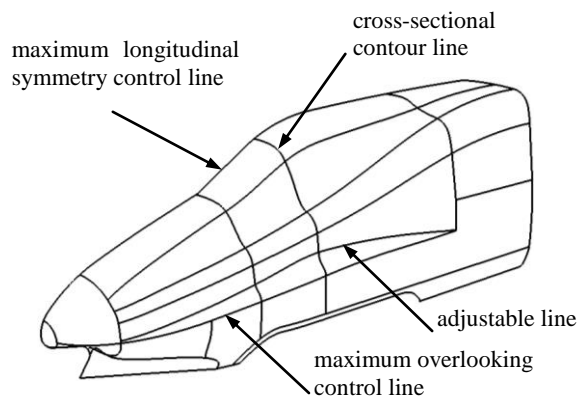

Figure 6. Main Control Lines of the Driver Cab

3.3 Generate Intermediate Control Lines of Driver Cab

Since the density of the main control lines is not high enough, they cannot be used to create the surface of driver cab directly, but need to generate some intermediate control lines appropriately in "Free Style" workbench of CATIA software. The method of generating intermediate control lines is firstly arraying the xz plane by unequal distance, and principle of the distance is that it can be smaller if the surface shape of an area changes a lot; while larger if the surface shape of an area only changes a little. The adding

planes intersect with the main control lines into a series of intersections，which expressed by $p_{i,j}$ （$i = 1, 2 \cdots, m$; $j = 1, 2 \cdots, n$）. The intermediate control lines represented by L_i （$i = 1, 2 \cdots, m$） of driver cab are formed by connecting the intersections with NURBS curve and is shown in Figure 7. The curve densification of yz plane direction is completed by the same steps as the xz direction, so the driver cab liking a spatial network structure is formed by a group of control lines and is shown in Figure 8.
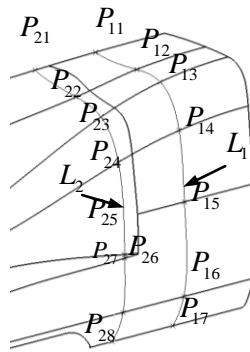

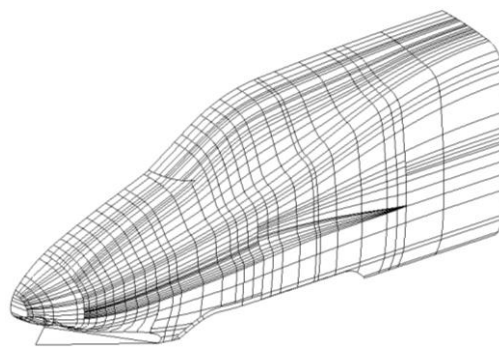**Figure 7. Intermediate Control Lines of the Driver Cab**

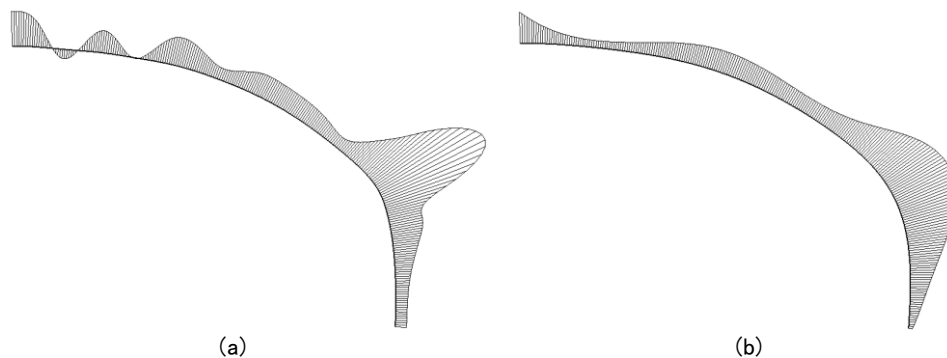**Figure 8. Control Lines of the Driver Cab**

Figure 9. Comparison In Curvature Comb Of NURBS Line: (A) Original Control Line (B) Optimized Control Line.

After the previous steps, now we can create the surface of the driver cab. Firstly, all the netlike control lines should be disconnected at the intersections, thus plenty of space grids, which are independent to each other, are formed, and then a large number of NURBS

surfaces are generated by padding all the grids. The half model of the driver cab is finished after the step of setting all the NURBS surfaces into tangency relation. The complete model is accomplished by a mirror operation based on the original half and headlight, front window, side doors can be created by segmentation and combination. The finished model of driver cab is shown in Figure 10.

Figure 10. Surface Model of the Driver Cab

3.4 Compartment Design and Virtual Assembly of the Head Car

A large number of wind tunnel experiments showed that the best cross section shape of compartment is drum if a train has a better aerodynamic performance level. We can depict the compartment as follows: the roof is a circular arc and both the upper part and the under part of sidewall incline inward and connected with roof and chassis by a circular arc, respectively. We set the angle of inclination on the upper part of sidewall is 4° and under part is 2°, and the radius of circular arc of roof is 400mm. The distance between the bottom of compartment and the railway track is 150mm, and the total area of the cross section is $11.3m^2$. The finished sketch is shown in Figure 11. The outer shape of the compartment is stretched by this sketch, and the side windows and side doors are finished by segmentation and combination.
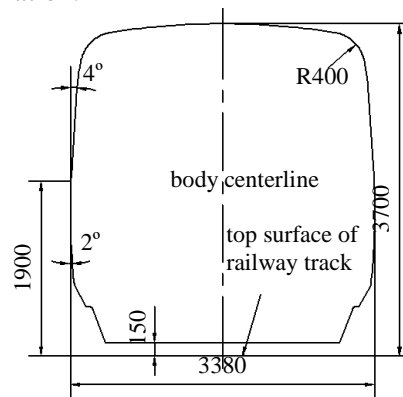

Figure 11. Cross-Section Of Compartment (Unit:Mm)

In the virtual environment, the head car is assembled with the driver cab and the compartment, which created in previous steps by surface adaption and aligning operation. We paint color on the model in order to make it artistic. The complete EMU head car surface model is shown in Figure 12.
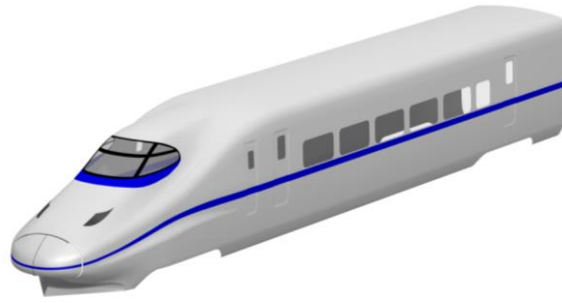
Figure 12. Surface Model of Head Car

The basic dimensions of the head car are listed in Table 2.

Table 2. Basic Dimensions of Head Car (Unit: M)

Position	Length	Width	Height
driver cab	9.5	3.38	3.7
compartment	16.2	3.38	3.7
head car	25.7	3.38	3.7

Both wind tunnel experiments and numerical simulations proved that for different EMU type, the bigger slenderness ratio of head car is, the less air resistance appears, so does the pressure wave when EMU passing each other[16]. To evaluate the aerodynamic performance of the head car with different shapes, the scholars usually take λ_L as the slenderness ratio of the head car，which is defined as follows:

$$\lambda_L = \frac{L}{\sqrt{S/\pi}} \tag{7}$$

In formula (7), L is the length of streamlined part of the head car, S is the area of cross section. We get the slenderness ratio involved in this passage λ_L =5.0 by calculating, which satisfies the common basic requirement that the slenderness ratio of high-speed EMU is no less than 3.0, namely $\lambda_L \geq$3.0.

4. Static Smoothness Evaluation of Head Car

Because a smooth surface can effectively eliminate or delay air boundary stripping and vortex generating, it is helpful to improve the aerodynamic performance of the vehicle. It needs to evaluate the surface smoothness of the head car when its surface model is completed and general methods include multiple sectional curvature comb and reflection lines [17].

4.1 Multiple Section Curvature Combs Method

Curvature comb is the vector indication of bending degree of the measured curve, which is helpful for intuitively evaluating the curve's smoothness. The method of multiple section curvature combs adopts several parallel planes cutting the surface, and then evaluates the curvature distribution of the intersecting lines of the measured surface. We can judge the quality of the surface by observing the changes of the intersecting lines curvature. For example, whether surface is reverse convex, whether there are gaps during surface joints, the maximum or minimum curvature value distribution and so on.

We add 5 parallel planes, which the distance between each other is 650mm to the

driver cab along its longitudinal direction and the curvature combs of intersecting lines are shown in Figure 13.
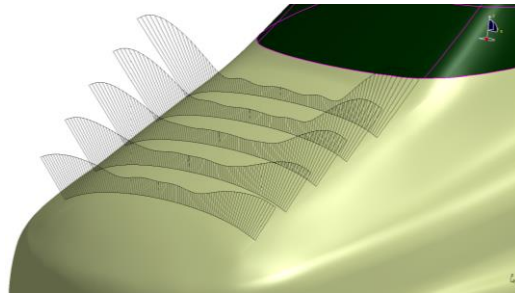

Figure 13. Multiple Section Curvature Combs Of Driver Cab

As can be seen from Figure 13, all of the curvature combs of the driver cab point to the same side, which indicates that the entire surface is purely convex. Meanwhile, observed by enlargement, nor curvature combs of the total surface appear inflection point and mutation, which indicates there is no gap between small NURBS surfaces so they match each other well.

4.2 Reflection Lines Method

The evaluation method of reflection lines firstly needs to create a group of equally spaced straight lines or curves outside of the surface model. Then fluorescent lamp is used to irradiate them on the measured surface vertically. The surface smoothness can be analyzed by observing the reflection lines. Considering the surface characteristics of the head car and the comprehensiveness of surface smoothness evaluation, we analyze both the front side and the profile of this head car, respectively. We adopt 20 concentric circles, which distance is 140mm at the front side and 20 straight lines which distance is 450mm at the profile. The reflection lines are shown in Figure 14.
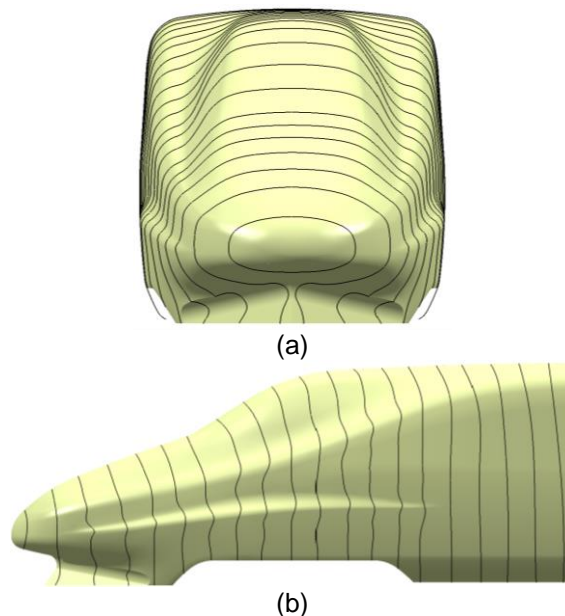

(a)

(b)

Figure 14. Reflection Lines of Head Car: (A) Front Side (B) Profile

Figure 14 shows that the reflection lines on both the front side and the profile of the head car are completely smooth and consecutive without any disconnection, mismatch

and disorder. The results indicate that there are no gap and irregular protrusions among all the NURBS surfaces and the surface smoothness conforms to the design requirements.

5. Aerodynamic Performance Evaluation of the Train in Flow Field

The streamlined design of high-speed EMU head car can significantly improve aerodynamic performance of train and effectively reduce air resistance when it runs at high speed [18]. We conduct the three-dimensional simulation of EMU flow field by CFD (computational fluid dynamics) calculation software ANSYS FLUENT12.0 in order to verify the aerodynamic performance of the streamlined head car designed in this paper. Compared with the traditional wind tunnel experiment, dynamic experiment and real vehicle test, the application of CFD technology can achieve the purpose of saving investment and shorten the design cycle [19]. In addition, in order to make the calculation more convenient, we do not consider the effect of the pantograph and the bogie on air resistance temporarily.

5.1 Size and Mesh of the Flow Field

The size of flow field is characterized by the total length of a three marshalling train, i.e. head car (L_1=25.7m), middle car (L_2=25.0m) and tail car (L_3=25.7m), so L=25.7+25.0+25.7=76.4m. The calculating flow field includes four dimensions, the inflow direction is 1L, outflow direction is 2L, width direction is 2L and height direction is 1L. Stream velocity is set to V=250km/h, outside air temperature T is set to 288K and atmospheric pressure is as the same as the standard atmospheric pressure. The boundary conditions are set as follows: the inflow boundary, the outflow boundary and the top boundary are non-reflecting boundary, the train body is no-slip wall boundary, the ground is set to moving wall and its speed is the same as the stream velocity [20]. In order to improve the convergence speed, unstructured grids are adopted in calculation area i.e. the meshes that near the train are refined and the remaining region are sparse. The total number of flow field meshes is 3.64 million approximately. The calculating area of the train is shown in Figure 15.
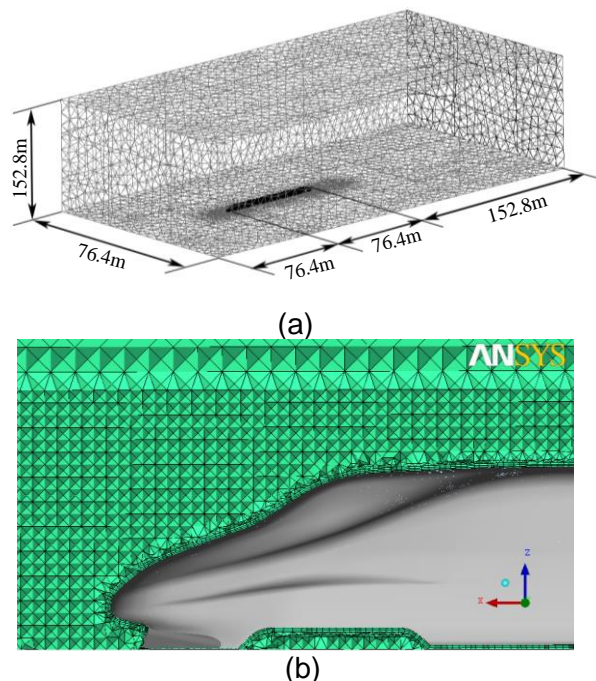

(a)

(b)

Figure 15. Calculating Area Meshes of the Flow Field: (a) overall meshes

(b) part meshes

5.2 Air Trajectories Analysis of the Flow Field

In this paper, the simulation condition is open air, so we employ incompressible unsteady flow to describe the flow field and adopt standard k-ε turbulence model to describe the flow field, relevant control equations are defined as follows[21]:

$$\frac{\partial u_i}{\partial x_i} = 0 \tag{8}$$

$$\rho u_j \frac{\partial u_i}{\partial x_j} = -\frac{\partial p}{\partial x_i} + \frac{\partial}{\partial x_j}\left[(\mu + \mu_t)\left(\frac{\partial u_i}{\partial x_j} + \frac{\partial u_j}{\partial x_i}\right)\right] \tag{9}$$

$$\frac{\partial(\rho k u_i)}{\partial x_i} = \frac{\partial}{\partial x_j}\left[\left(\mu + \frac{\mu_t}{\sigma_k}\right)\frac{\partial k}{\partial x_j}\right] + \mu_t \frac{\partial u_j}{\partial x_i}\left(\frac{\partial u_j}{\partial x_i} + \frac{\partial u_i}{\partial x_j}\right) - \rho\varepsilon \tag{10}$$

$$\frac{\partial(\rho \varepsilon u_i)}{\partial x_i} = \frac{\partial}{\partial x_j}\left[\left(\mu + \frac{\mu_t}{\sigma_\varepsilon}\right)\frac{\partial \varepsilon}{\partial x_j}\right] + C_1 \mu_t \frac{\varepsilon}{k}\frac{\partial u_j}{\partial x_i}\left(\frac{\partial u_j}{\partial x_i} + \frac{\partial u_i}{\partial x_j}\right) - C_2 \rho \frac{\varepsilon^2}{k} \tag{11}$$

In formula (8) to (11), u_i, u_j represent the speed of flow field around the train, x_i, x_j represent coordinate component, ρ represents the density of air, p represents pressure, μ represents aerodynamic viscosity coefficient of air ; μ_t represents viscosity coefficient of turbulent and $\mu_t = C_\mu \rho k^2 / \varepsilon$, k represents turbulent kinetic energy, ε represents the dissipation rate of the turbulence, C_u represents turbulence constant, $C_1, C_2, \sigma_k, \sigma_\varepsilon$ represent empirical coefficients, respectively. The finite volume method is used to discrete the control equations and the air trajectories of streamlined train in flow field are shown in Figure 16.
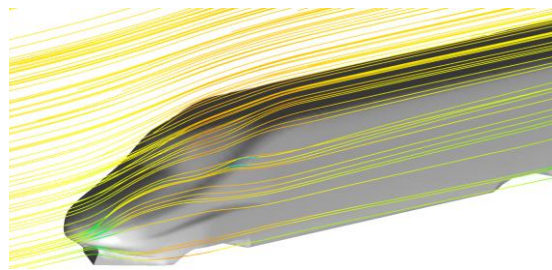

Figure 16. Air Trajectories of Streamlined Train in Flow Field

As can be seen from Figure 16, the air trajectories are smooth and steady when the air flows through the head car. The air trajectories do not form horizontal or vertical vortex, but show a natural and smooth flow state. This fully shows that there are no irregular protrusions on the head car outer surface. The simulation result fully proves that the head car designed in this paper has a better quality.

5.3 Air Resistance Comparison of Different EMU

At present, a certain number of quasi-streamlined EMU are still used in the high-speed railways of China. The main characteristics of quasi-streamlined EMU head car is that its length of driver cab is shorter of which the slenderness ratio (λ_L) is less than 3.0. Now we adopt the same marshalling form, flow field sizes and calculation method (V=250km/h).

The surface pressure contour and air trajectories of the head car of streamlined train and quasi-streamlined one are calculated respectively and shown in Figure17.
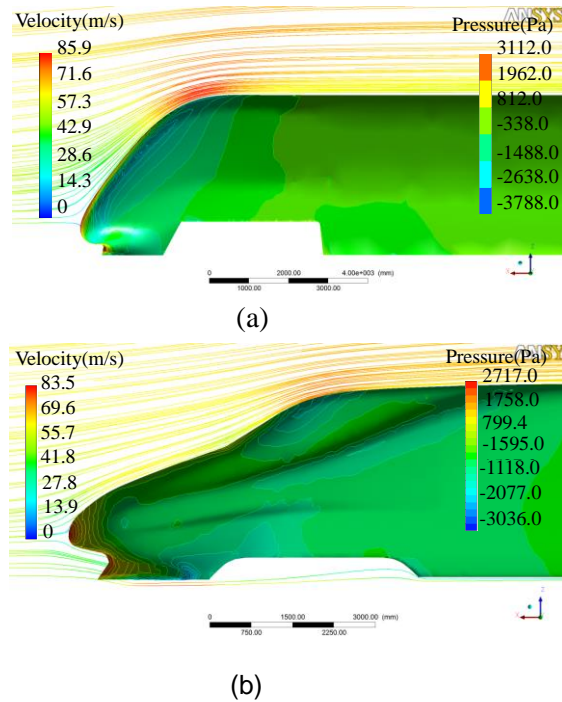

(a)

(b)

Figure 17. Comparison in Surface Pressure Contour and Air Trajectories: (A) Quasi-Streamlined Head Car (B) Streamlined Head Car

Figure 17 shows that the maximum air trajectories velocity of the two type head cars both appear at the joint of the driver cab and the compartment in which the result of quasi-streamlined train is 85.9m/s and the streamlined one is 79.3m/s. The maximum pressure occurs in the nasal tip of the head car in both type EMU, the result of the quasi-streamlined train is 3112.0pa and the streamlined one is 2717.0pa. The calculation results above indicate that the streamlined train has a better aerodynamic performance than quasi-streamlined one.

In order to verify the aerodynamic performance of streamlined train more comprehensively, now we set the stream velocity is 50 km/h,100km/h,150km/h, 200km/h, 250km/h and 300km/h respectively, then adopt the same method to calculate the air resistance of quasi-streamlined train and streamlined one. According to the results of previous studies, the total air resistance of high-speed trains includes differential pressure resistance, frictional resistance and interference resistance. The differential pressure resistance is caused by the pressure difference between head car and tail car, air viscosity which is acting on the train surface induces the frictional resistance and the interference resistance is caused by the protrusions of trains (such as bogie, doors, windows, chassis and roof equipments). Because the two type trains assembly the same bogie and roof equipments, we may only calculate differential pressure resistance and frictional resistance. The calculating results are listed in Table 3.

Table 3. Calculating Results of the Air Resistance of Quasi-Streamlined Train and Streamlined One at Different Velocities

Velocity（km/h）	Train type	Differential pressure resistance（N）	Frictional resistance（N）	Total air resistance（N）
50	quasi-streamlined	574.3	208.9	783.2

	streamlined	451.2	151.5	602.7
100	quasi-streamlined	1772.5	638.0	2410.5
	streamlined	1221.5	518.3	1739.8
150	quasi-streamlined	3963.1	1316.1	5279.2
	streamlined	2514.0	1383.1	3897.1
200	quasi-streamlined	6915.9	1897.6	8813.5
	streamlined	3754.3	2320.1	6074.4
250	quasi-streamlined	11035.3	3435.4	14470.7
	streamlined	6006.3	3498.3	9504.6
300	quasi-streamlined	15927.9	4972.5	20900.4
	streamlined	8210.1	4892.7	13102.8

In order to describe the total air resistance at different velocities of the two type trains intuitively, a velocity-air resistance-fitting curve is drawn and shown in Figure 18.
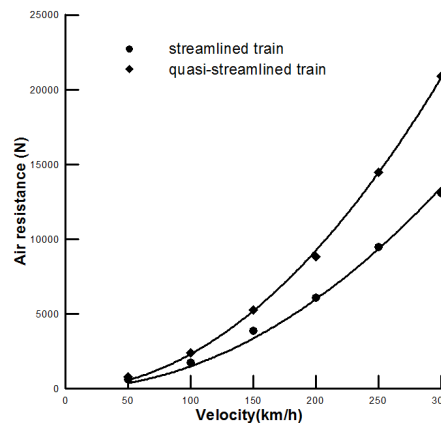
Figure 18. Velocity-Air Resistance Fitting Curve of Quasi-Streamlined Train and Streamlined One

From Figure 18, we can see that the velocity-air resistance fitting curves of the two type trains are both quadratic parabola, namely the total air resistance is proportional to the square of the train velocity. The total air resistance of streamlined train reduces by 23.0% at the velocity of 50km/h, 27.8% at 100km/h, and 26.2% at 150km/h, 31.1% at 200km/h, 34.3% at 250km/h and 37.3% at 300km/h compared with the quasi-streamlined one. The above data show that the streamlined head car has obvious effect on lower air resistance.

6. Conclusions

In this paper, the digital design process of streamlined EMU head car outer surface is completed by adopting NURBS modeling method. Meanwhile, with the beneficial tool of curve curvature combs, the control lines, which are not smooth enough are found and be optimized. The static evaluation of head car indicates that the measured region is smooth, which fully shows the design method is correct. The air trajectories in the flow field of the streamlined EMU train are clear, which illustrates that the head car has a better surface quality. In addition, the total air resistance of the streamlined train and quasi-streamlined one is calculated at different running velocities. The calculating results indicate that the aerodynamic performance of streamlined train is significantly improved due to its optimized shape of head car. The digital model of the streamlined EMU head car is an important technical reference for the subsequent manufacturing of the outer skin plates and frame installation. If some researchers will continue to study the results in this paper, further in-depth studies research could be done about the above problems.

Acknowledgements

References:

[1] C. Baker, "The flow around high speed trains", Journal of Wind Engineering and Industrial Aerodynamics, vol. 98, no. 6, **(2010)**, pp. 266−298.

[2] J. Schetz, "Aerodynamics of high-speed train", Annual Review of Fluid Mechanics, vol. 33, **(2001)**, pp. 371-414.

[3] E. Catmull and J. Clark, "Recursively generated B-spline surfaces on arbitrary topological meshes", Computer Aided Geometric Design, vol. 16 no. 6, **(1978)**, pp. 350−355.

[4] L. Pieg1, "Modifying the shape of rational B-spline", Curve. Computer Aided Design, vol. 21, no. 5, **(1989)**, pp. 9−18.

[5] C. Au and M. Yuen, "Unified approach to NURBS curve shape modification", Computer Aided Design, vol. 34, no. 27, **(1995)**, pp. 85−93.

[6] J. M. Zheng, J. M. Chan and I. Gibson, "A new approach for direct manipulation of free-form curve", Computer Graphics Forum, vol. 17, no. 3, **(1998)**, pp. 28−34.

[7] N. Cherpeau, G. Caumon and B. Levy, "Stochastic simulations of fault networks in 3D structural modeling", Comptes Rend us Geoscience, vol. 342, no. 9, **(2010)**, pp. 687−694.

[8] T. Ozbolat and B. Koc, "Multi-directional blending for heterogeneous objects", Computer Aided Design, vol. 43, no. 8, **(2011)**, pp. 863−875.

[9] S. Huang, W. B. Song, F. Zhou, J. H. Wang and M. H. Zhang, "Aerodynamic design of forward fuselage using NURBS with engineering constraints" , Acta aerodynamic sinica, vol. 30, no. 3, **(2012)**, pp. 394−399.

[10] K. Y. Hu, Y. M. Lu and Y. Ding, "Research on deep-vee trimaran stability based on the non-uniform rational B-spline method", Journal of Harbin Engineering University, vol. 32, no. 10, **(2011)**, pp. 1273−1277.

[11] B. Shen, D. J. Qi, L. L. Fan and Zh. H. Zhu, "High-speed adaptive interpolation algorithm based on NURBS fitting for micro sections", China Mechanical Engineering, vol. 23, no. 15, **(2012)**, pp. 1825−1829.

[12] M. Lounsbery, R. T. De and J. Warren, "Multiresolution analysis for surfaces of arbitrary topological type", ACM Transaction on Graphics, vol. 16, no. 1, **(1997)**, pp. 34−73.

[13] H. P. Moreton and C. H. Sequin, "Functional optimization for fair surfaces design", Computer Graphics, vol. 26, no. 2, **(1992)**, pp. 167-175.

[14] I. T. Ozbolat and B. Koc, "Multi-directional blending for heterogeneous objects", Computer Aided Design, vol.43, no.8, **(2011)**, pp.863-875.

[15] M.Bertram, "Single-knot wavelets for non-uniform B-splines", Computer Aided Geometric Design, vol. 22, no. 9, **(2005)**, pp. 849-864.

[16] C. J. Baker, J. Jones, F. Lopez and J. munday, "Measurements of the cross wind forces on trains", Journal of Wind Engineering and Industrial Aerodynamics, vol. 92, no. 7, **(2004)**, pp. 547-563.

[17] N. Guid, C. Oblonsek and B. Zalik, "Surface interrogation methods", Computers & Graphics, vol. 19, no. 4, **(1995)**, pp. 557-574.

[18] R. Raghunathan, S. Kim and T. Setoguchi, "Aerodynamics of high-speed railway train", Progress in Aerospace Sciences, vol. 38 no. 6, **(2002)**, pp. 469-514.

[19] A. Jameson, "Aerodynamic design via control theory", Journal of Scientific Computing, vol. 13, no. 3, **(1988)**, pp. 233-260.

[20] H. Hemida and S. Krajnovic, "LES study of the influence of the nose shape and yaw angles on flow structures around trains" , Journal of Wind Engineering and Industrial Aerodynamics, no. 98, **(2010)**, pp. 34-46.

[21] S. B. Yao, D. L. Guo and G. W. Yang, "Three-dimensional aerodynamic optimization design of high-speed train nose based on GA-GRNN", Science China Technology Sciences, vol. 55, no. 11, **(2012)**, pp. 3118-3130.

Author

Zhenfeng Wu was born in Heilongjiang, China. He received his bachelor's degree from Shijiazhuang Railway Institute. Now he is a PhD Candidate and an associate professor of the School of Mechanical & Electrical Engineering in Lanzhou Jiaotong University. His main research interests include digital design of complex surface products, aerodynamic analysis of high-speed trains and mechanical properties analysis of surface sheet metal during its forming process.